Ind. J. Pharm. Edu. Res., 2027; 61(1):10.5530/ijper.20262532.
https://www.ijper.org

Original Article

Multi-Omics and *in silico* Study of Anticancer Potential of *Salvia miltiorrhiza* (Danshen in Traditional Chinese Medicine) in Liver Cancer Cells: Metabolomics, Proteomics, Transcriptomics, *In silico* Molecular Docking, and *in vitro* Analysis

Yang Xu[1,#] , Yan Wang[2,#], Yuchao Mao[3], Yingli Ma[4,*]

[1]Department of Integrated Traditional Chinese and Western Medicine, Wuhan Third Hospital, Tongren Hospital of Wuhan University, Wuhan, Hubei, CHINA.
[2]Department of Procurement and Supply, Yantai Qishan Hospital, Yantai Shandong, CHINA.
[3]Department of Blood Transfusion, Chifeng City Cancer Hospital, Chifeng Inner Mongolia, CHINA.
[4]Department of Orthopaedics, Xianyang Hospital of Yan'an University, Xianyang, Shaanxi, CHINA.
[#]These authors contributed equally to this work.

ABSTRACT

Background: Liver cancer remains a leading cause of cancer-related deaths worldwide. Traditional Chinese Medicine (TCM), including *Salvia miltiorrhiza* (Danshen), has demonstrated potential anticancer properties. This study explores the molecular mechanisms underlying the therapeutic effects of Danshen on liver cancer using network pharmacology, enrichment analysis, molecular docking, and *in vitro* validation. **Materials and Methods:** Phytochemical constituents of Danshen were systematically screened from the TCMSP database, applying filters for oral bioavailability (≥55%), drug-likeness (≥0.18), and CaCo-2 permeability (≥-0.4). Compound toxicity was evaluated using ProTox-3.0. SwissTargetPrediction and SuperPred databases were utilized for target prediction of active compounds, while liver cancer gene targets were obtained from GeneCards. Overlapping targets were subjected to Protein-Protein Interaction (PPI) network analysis. Functional annotation using GO and KEGG pathway enrichment was performed to identify involved biological processes. Molecular docking using CB-Dock2 assessed the binding affinities of key compounds to target proteins. Gene expression and immune infiltration analyses were conducted using GEPIA2 and TIMER, respectively. *In vitro* validation employed HepG2 cells for MTT cell viability, clonogenic survival, Annexin V/PI apoptosis assays, and Western blotting for STAT3, HSP90AA1, and HSP90AB1 protein expression. **Results:** Screening identified 202 compounds from Danshen, reduced to 14 by pharmacokinetic filters, and 8 after toxicity and target prediction. Target analysis found 115 potential proteins, with 74 overlapping liver cancer genes. Protein interaction analysis highlighted 10 key hub genes, including STAT3, HSP90AA1, and HSP90AB1. Enrichment analysis indicated roles in PI3K-Akt, HIF-1, and PD-L1/PD-1 pathways. Molecular docking showed that Compound A bound strongly to STAT3 (-7.0 kcal/mol), HSP90AA1 (-9.0), and HSP90AB1 (-9.2), while Przewalskin b showed similar strong affinities (-7.5, -9.1, -9.1 respectively), suggesting potent inhibitory interactions with these oncogenic proteins. Key genes were overexpressed in liver cancer and associated with poor prognosis and immune cell infiltration. Laboratory assays confirmed cytotoxicity, reduced clonogenicity, induced apoptosis, and downregulated STAT3, HSP90AA1, and HSP90AB1. **Conclusion:** In conclusion, Danshen exhibits significant anti-liver cancer potential through modulation of key oncogenic pathways. Further *in vivo* and clinical validation is warranted to establish its therapeutic viability.

Keywords: Traditional Chinese medicine, Toxicity analysis, Tumor microenvironment, Integrative oncology, Immune infiltration.

Correspondence:
Dr. Yingli Ma
Department of Orthopaedics, Xianyang Hospital of Yan'an University, Xianyang, Shaanxi-712000, CHINA.
Email: yinglimayin992@hotmail.com
ORCID: 0009-0009-2046-7808

Received: 06-05-2026;
Revised: 29-06-2026;
Accepted: 10-08-2026.

DOI: 10.5530/ijper.20272532

Copyright Information :
Copyright Author (s) 2027 Distributed under Creative Commons CC-BY 4.0

Publishing Partner : Manuscript Technomedia. [www.mstechnomedia.com]

INTRODUCTION

Globally, liver cancer is a highly lethal form of cancer characterized by high heterogeneity, aggressive progression, and limited therapeutic efficacy.[1] Hepatocellular Carcinoma (HCC), comprising over 85% of all instances, arises predominantly in the context of chronic liver diseases, including Metabolic

dysfunction-Associated Steatohepatitis (MASH), and hepatitis B/C infections, cirrhosis.[2] Despite advancements in surgical resection, immunotherapy, and targeted therapies like sorafenib, the five-year survival rate remains dismal (<20%), underscoring the urgent prerequisite for novel overcoming strategies.[3] Tumor microenvironment complexity, drug resistance, and late-stage diagnosis further complicate management, necessitating interdisciplinary approaches integrating molecular insights and innovative drug discovery paradigms to address unmet clinical needs.

Network pharmacology, a systems biology-driven paradigm, has developed as a transformative force in drug-discovery by elucidating the polypharmacological interactions of multi-component therapeutics with disease networks.[4,5] Unlike reductionist single-target approaches, this discipline employs computational tools to map compound-target-disease networks, enabling the identification of synergistic mechanisms, off-target effects, and holistic therapeutic profiles. Its application is revolutionizing traditional medicine systems, including TCM, which emphasizes multi-herb formulations targeting "body network" imbalances.[5] By integrating omics data, cheminformatics, and AI-driven algorithms, network pharmacology deciphers the "multi-component, multi-target, multi-pathway" framework of TCM, bridging empirical knowledge with mechanistic validation.[6] For instance, *Salvia miltiorrhiza* exhibits therapeutic potential through integrated metabolomics, transcriptomics, and network pharmacology approaches. Bioactive compounds identified via metabolomics interact with key molecular targets revealed by transcriptomic analysis, regulating pathways such as INS/SRC/IL6, Src/Akt, and RhoA.[7,8] These mechanisms contribute to anti-cancer, anti-platelet, and anti-thrombotic effects, highlighting its multi-target, systems-level pharmacological actions. Collaborative efforts to curate TCM-specific databases (e.g., TCMSP, TCMID) and advances in multi-omics integration (pharmacogenomics, metabolomics) are enhancing predictive accuracy. As a convergence point of ethnopharmacology and cutting-edge bioinformatics, network pharmacology not only revitalizes traditional therapies but also redefines drug discovery paradigms, offering a scaffold for personalized, systems-level medicine in oncology, neurodegeneration, and immune disorders.

Salvia miltiorrhiza (Chinese Danshen), a key TCM herb, contains tanshinones and salvianolic acids with antioxidant, anti-inflammatory, and anti-fibrotic effects.[9-13] Traditionally used for “blood stasis” disorders like cirrhosis and ischemic injury, it shows hepatoprotective and anticancer activity. Tanshinone IIA induces apoptosis in hepatocellular carcinoma via PI3K/AKT/mTOR inhibition, while salvianolic acid B modulates TGF-β/Smad signaling, highlighting its potential in integrative liver cancer therapy.[14,15]

This study aims to systematically probe the mechanisms of action and bioactivity of Danshen against liver cancer by integrating network pharmacology predictions with experimental validation. Leveraging bioinformatics tools, we will construct compound-target-pathway networks to identify key phytochemicals and their interactomes within HCC-associated signaling cascades. Computational findings will be validated through *in vitro* assays (e.g., proliferation, apoptosis, migration in HCC cell lines). By elucidating Danshen's multi-target synergy and molecular crosstalk, this work seeks to establish a mechanistic foundation for its ethnomedical use, bridging TCM wisdom with contemporary oncology drug discovery.

MATERIALS AND METHODS

Phytochemical Screening

Phytochemical constituents of Danshen were systematically screened from the TCMSP database. The TCMSP database is a comprehensive resource for traditional Chinese medicine, integrating chemical, biological, and pharmacological data to study drug efficacy and mechanisms at a systems level (“https://tcmsp-e.com/tcmsp.php”). Compounds were filtered based on pharmacokinetic parameters: BioAva ≥55%, DL ≥0.18, and Caco-2 permeability ≤-0.4, ensuring selection of molecules with favorable absorption, distribution, and bioavailability profiles. The Veber’s criteria and Lipinski’s Rule of Five were applied to prioritize drug-like candidates. Redundant or non-bioactive compounds were excluded, yielding a refined library of Danshen-derived phytochemicals for subsequent analyses.

Toxicity Analysis

The toxicity profiles of screened compounds were evaluated using ProTox-3.0, a predictive tool for organ-specific toxicity (“https://tox.charite.de”). Hepatotoxicity, cytotoxicity, mutagenicity, and carcinogenicity were assessed via machine learning models trained on structural alerts and molecular descriptors.[16] Compounds were classified into toxicity classes (I-VI) based on predicted median Lethal Dose (LD_{50}) values and probability scores. Only molecules exhibiting negligible hepatotoxicity (class ≥IV, LD_{50} >500 mg/kg) and lacking mutagenic or carcinogenic alerts were retained, ensuring safety for further pharmacological investigation.

Target Prediction

Potential targets of Danshen phytochemicals were predicted using SwissTargetPrediction and SuperPred, with probability thresholds set at ≥0.7 (SwissTargetPrediction) and ≥70% (SuperPred) to ensure high-confidence interactions.[17,18] The SuperPred database uses machine learning to predict drug classification (ATC codes) and protein targets for chemical compounds based on molecular similarity, aiding in drug discovery and repurposing ("https://prediction.charite.de"). The SwissTargetPrediction database predicts potential protein targets for small molecules using structural similarity and machine learning, facilitating the identification of

IN PRESS

drug-target interactions "http://www.swisstargetprediction.ch". Both SuperPred and SwissTargetPrediction are used in network pharmacology to identify potential drug targets and interactions by analyzing molecular similarities and predicting binding affinities, enabling the construction of complex drug-target-disease networks to uncover therapeutic mechanisms and support drug development.

Targets were cross-referenced with liver cancer-associated genes from GeneCards (filtered by GeneCards Inferred Functionality Score [GIFtS] ≥0.7), prioritizing disease-relevant proteins ("https://www.genecards.org/"). Redundant entries were removed, and targets were standardized using UniProt IDs. This integrative approach identified a consolidated list of phytochemical-disease targets for network construction.

Network Construction

Common gene targets between Danshen phytochemicals and liver cancer were identified using Jvenn (intersection mode) and mapped to the STRING database to generate PPI networks.[19] The jVenn tool is an interactive JavaScript-based plugin for the jQuery library, designed to create dynamic Venn diagrams for comparing up to six lists of elements with customizable layouts and export options ("http://jvenn.toulouse.inra.fr"). Interactions were filtered by a confidence score ≥0.700, and unconnected nodes were removed to enhance network specificity. The resultant PPI network was visualized by imported into Cytoscape and topological analysis was achieved. Hub genes were identified using the CytoHubba degree algorithm, with the top 10 nodes ranked by MCC score designated as critical regulators of liver cancer pathogenesis.

Gene Ontology

Functional annotation of common targets was performed using the ShinyGO platform (v0.8).[20] The ShinyGO 0.80 website, a graphical tool for gene-set enrichment analysis with interactive pathway and network visualizations for over 14,000 species, is accessible at "http://bioinformatics.sdstate.edu/go/". Gene Ontology (GO) terms for Biological Processes (BP), Cellular Components (CC), and Molecular Functions (MF) were enriched with a False Discovery Rate (FDR) <0.05. Kyoto Encyclopedia of Genes and Genomes (KEGG) pathway analysis was conducted to map targets onto liver cancer-associated signaling cascades (e.g., PI3K-AKT, HIF-1, TNF-α). Enrichment results were exported as bubble plots and Excel Sheets, highlighting pathways with adjusted *p*-values <0.01 and gene counts ≥5.

Tumor Microenvironment Evaluation

The TIMER 2.0 database was employed for the assessment of correlation concerning hub genes and immune-cell-infiltration in liver cancer. The TIMER 2.0 website, a tool for analyzing tumor-infiltrating immune cells with advanced algorithms and interactive visualizations, is accessible at ("http://timer.cistrome.org/"). Tumor purity-adjusted Spearman's correlation coefficients were calculated for six immune cell types (B cells, CD4+ T cells, CD8+ T cells, neutrophils, macrophages, dendritic cells) across HCC cohorts from TCGA and GEO datasets. Hub genes exhibiting significant associations ($p<0.05$) with immune infiltration levels were flagged as potential modulators of the Tumor Microenvironment (TME), informing their roles in immunomodulation and therapeutic response.

Molecular docking

Execution of molecular docking was performed for Compound A and przewalskin b against the hub genes STAT3, HSP90AA1, and HSP90AB1 using CB-Dock2. The CB-Dock2 website, an advanced tool for protein-ligand blind docking with cavity detection, AutoDock Vina integration, and homologous template fitting for precise binding site prediction, is accessible at "https://cadd.labshare.cn/cb-dock2/".[21] The protein structures for STAT3, HSP90AA1, and HSP90AB1 were downloaded from the RCSB PDB database bearing PDB IDs 6NUQ, 5NYH, and 1UYM. The compounds were prepared using ChemDraw, and the downloaded PDB files were processed and prepared using Discovery Studio. The docking results were analyzed, and the 2D visualization was executed using Discovery Studio to show different binding interactions between the compounds and hub targets.

Extraction of Aerial Parts of Danshen Using a Soxhlet Extractor

The aerial parts of Danshen (*Salvia miltiorrhiza*) were carefully washed with distilled water to eliminate any impurities and dried at 40°C for 48 hr. The plant was identified by Dr Wei Yuan (Xianyang Hospital of Yan'an University, Xianyang Shaanxi, CHINA) (voucher number-YUXS-880). The dried material was finely ground using a mechanical grinder. For the extraction process, 50 g of the powdered material was placed into a cellulose thimble and loaded into a Soxhlet extractor. The extraction flask was filled with 300 mL of ethyl acetate, and the apparatus was set up. The solvent was heated to 77°C under reflux, and the extraction was conducted for 3 hr, ensuring continuous solvent cycling. Collecting the solvent-herb combination after extraction allowed us to filter out any solid particles using Whatman No. 1 filter paper. The residual extract was freeze-dried to produce a dry powder, and the ethyl acetate was then evaporated under reduced pressure using a rotary evaporator set at 40°C. It was kept at -10°C until it was required again for further experimentation.

Chemicals, Reagents, Equipment, and Antibodies

Dulbecco's Modified Eagle Medium (DMEM), Fetal Bovine Serum (FBS), penicillin-streptomycin, trypsin-EDTA, Phosphate-Buffered Saline (PBS), Dimethyl Sulfoxide (DMSO), MTT reagent, paraformaldehyde, and crystal violet were all purchased from Sigma-Aldrich (Merck KGaA, Darmstadt, Germany). Danshen extract stock solutions were prepared in

IN PRESS

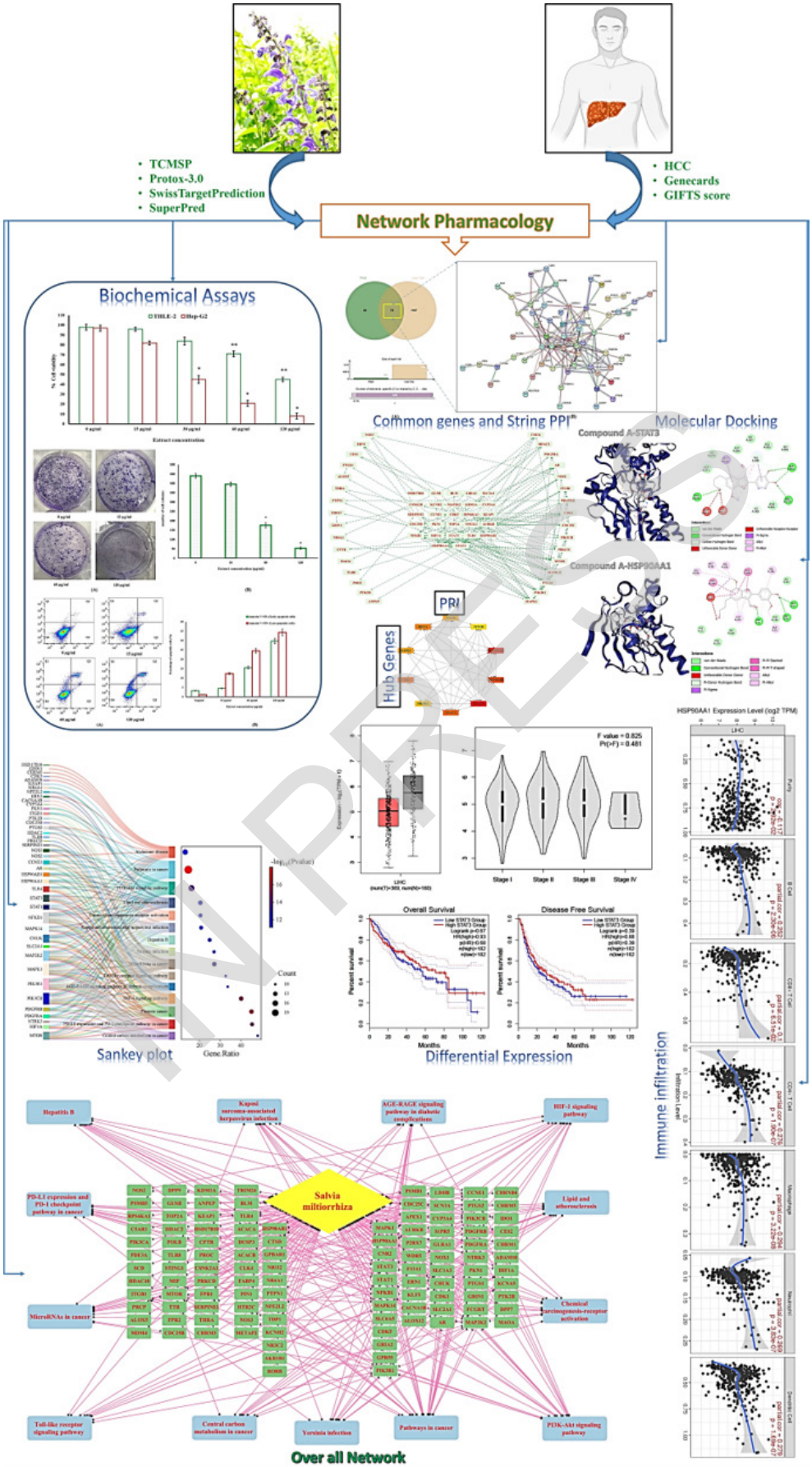


Figure 1: Flow chart revealing the complete workflow of the study.

IN PRESS

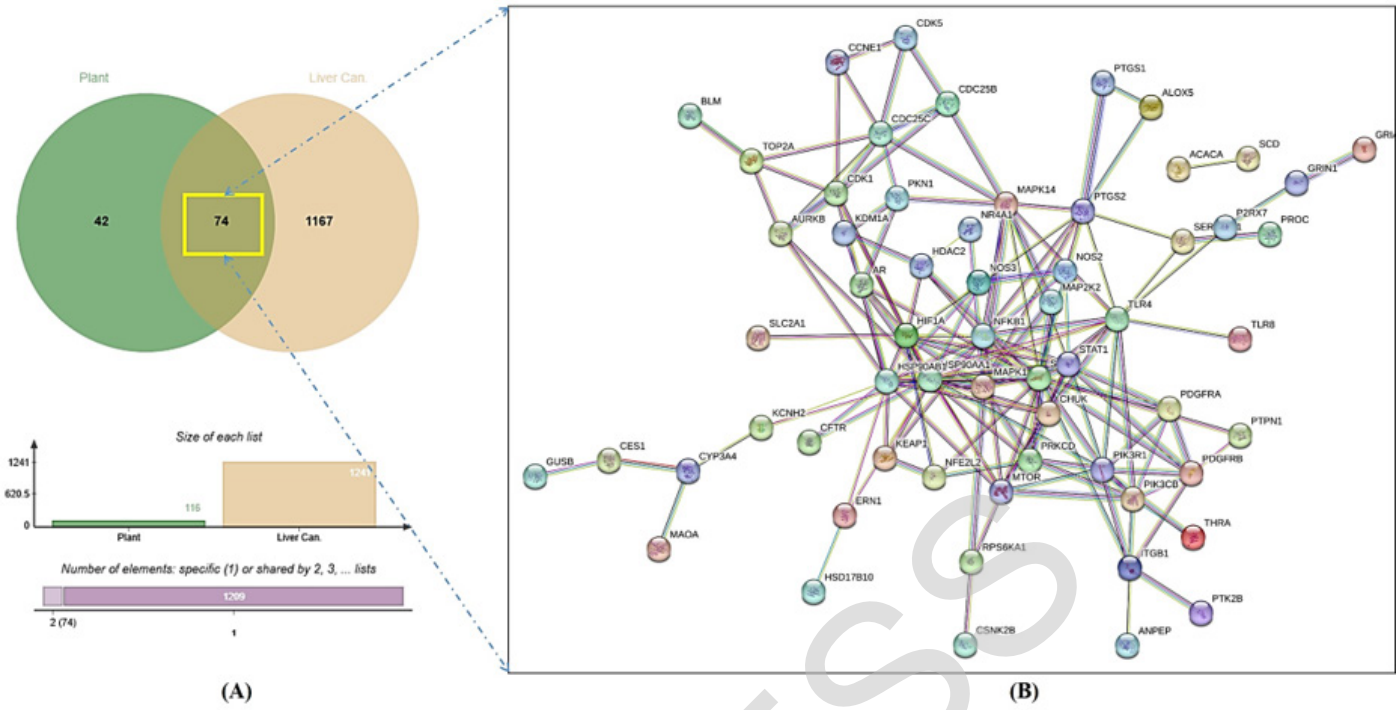


Figure 2: A: Common targets associated with liver cancer identified from the eight compounds screened. B: PPI network of 74 common targets generated using the STRING database, showing 74 nodes and 160 edges with an average node degree of 4.32.

DMSO (Sigma-Aldrich). The MTT absorbance was measured using a microplate reader, model ELx800 (BioTek Instruments, Inc., Winooski, VT, USA). Flow cytometric analysis for apoptosis was performed on a BD FACSCalibur flow cytometer (BD Biosciences, San Jose, CA, USA). Western blotting utilized a Mini-PROTEAN Tetra Cell system and a Trans-Blot Turbo Transfer System (Bio-Rad Laboratories, Inc., Hercules, CA, USA). Primary antibodies against STAT3, HSP90AA1, HSP90AB1, and β-actin, and HRP-conjugated secondary antibodies were obtained from Cell Signaling Technology (Danvers, MA, USA). Protein quantification was performed using Pierce™ BCA Protein Assay Kit (Thermo Fisher Scientific, Waltham, MA, USA). Enhanced Chemiluminescence (ECL) detection was carried out using SuperSignal™ West Pico PLUS substrate (Thermo Fisher Scientific). ImageJ software (National Institutes of Health, Bethesda, MD, USA) was used for densitometric analysis of blots.

Cell Culture

THLE-2 (normal liver) and HepG2 (hepatocellular carcinoma) cell lines were obtained from the American Type Culture Collection (ATCC, Manassas, VA, USA) and cultured in Dulbecco's Modified Eagle Medium (DMEM) supplemented with 10% Fetal Bovine Serum (FBS) and 1% penicillin-streptomycin. The cells were maintained at 37°C in a humidified incubator with 5% CO_2. Upon reaching 80-90% confluency, the cells were subcultured using 0.25% trypsin-EDTA. All experiments were performed using cells in the logarithmic growth phase.

MTT Assay for Cytotoxicity against THLE-2 and HepG2 Cells

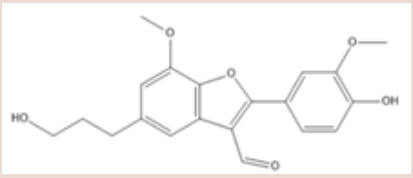
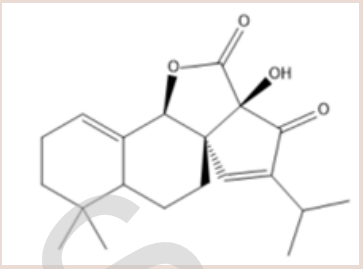
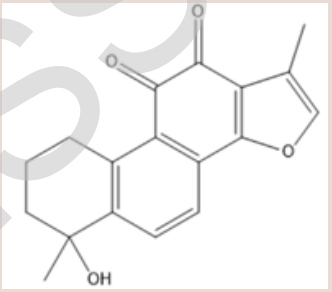
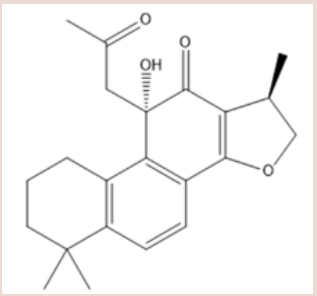
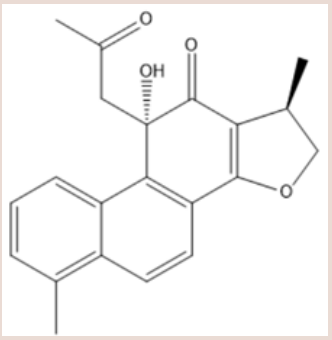
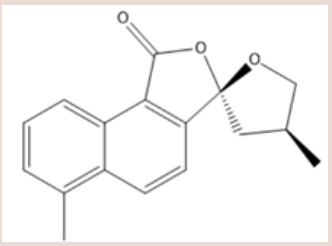
The THLE-2 and HepG2 cells were seeded in 96-well plates at a density of 5×10^3 cells/well in DMEM supplemented with 10% FBS and incubated for 24 hr at 37°C in a 5% CO_2 environment. Stock solutions of Danshen extract were prepared in DMSO, ensuring the final DMSO concentration did not exceed 0.1%, and diluted in media to achieve concentrations of 0 (control), 15, 30, 60, and 120 µg/mL. The media in the wells was replaced with the treatment solutions, and the cells were incubated for 24 hr. After incubation, 20 µL of MTT reagent (5 mg/mL in PBS) was added to each well, and the plates were incubated for an additional 4 hr. The media was carefully removed, and the formazan crystals were dissolved in 150 µL of DMSO. The absorbance was measured at 570 nm using a microplate reader, and cell viability was calculated as a percentage relative to the untreated control.

Clonogenic Assay for HepG2 Cells

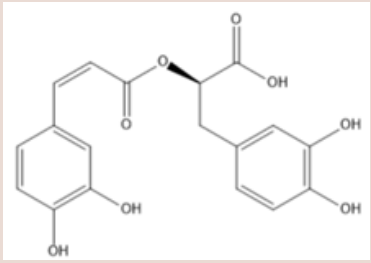
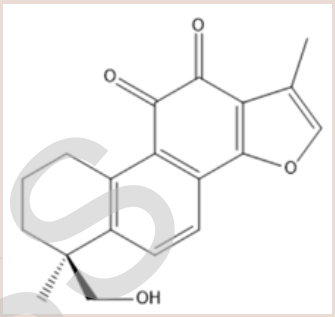
HepG2 cells were seeded at a density of 500 cells/well in 6-well plates and allowed to adhere for 24 hr. The cells were then treated with Danshen extract at concentrations of 0, 15, 60, and 120 µg/mL for 48 hr. After treatment, the media was replaced with fresh drug-free media, and the cells were incubated for 14 days to allow colony formation. The colonies were fixed with 4% paraformaldehyde for 15 min, stained with 0.5% crystal violet for 30 min, and rinsed with PBS. The plates were air-dried, and colonies consisting of more than 50 cells were counted using a

IN PRESS

Table 1: The structure and Smiles of eight bioactive phytochemicals screened from Danshen.

Sl. No.	Compounds	Smiles	Structure
1.	Compound A=2-(4-hydroxy-3-methoxyphenyl)-5-(3-hydroxypropyl)-7-methoxy-3-benzofurancarboxaldehyde	"COC1=CC(=CC2=C1OC(=C2C=O)C3=CC(=C(C=C3)O)OC)CCCO"	
2.	Przewalskin b	"CC(C)C1=C[C@]23CCC4C(=CCCC4(C)C)[C@H]2OC(=O)[C@@]3(C1=O)O"	
3.	Przewaquinone c	"CC1=COC2=C1C(=O)C(=O)C3=C2C=CC4=C3CCCC4(C)O"	
4.	Danshenol B	"C[C@H]1COC2=C1C(=O)[C@@](C3=C2C=CC4=C3CCCC4(C)C)(CC(=O)C)O"	
5.	Danshenol A	"C[C@H]1COC2=C1C(=O)[C@@](C3=C2C=CC4=C(C=CC=C43)C)(CC(=O)C)O"	
6.	Epidanshenspiroketallactone	"C[C@H]1C[C@@]2(C3=C(C4=CC=CC(=C4C=C3)C)C(=O)O2)OC1"	

IN PRESS

Sl. No.	Compounds	Smiles	Structure
7.	Compound B=(2R)-3-(3,4-dihydroxyphenyl)-2-[(Z)-3-(3,4-dihydroxyphenyl) acryloyl]oxy-propionic acid	"C1=CC(=C(C=C1C[C@H](C(=O)O)OC(=O)/C=C\C2=CC(=C(C=C2)O)O)O)O"	
8.	Compound C=(6S)-6-(hydroxymethyl)-1,6- dimethyl-8,9-dihydro-7H-naphtho[8,7- g]benzofuran-10,11-dione	"CC1=COC2=C1C(=O)C(=O)C3=C2C=CC4=C3CCC[C@]4(C)CO"	

colony counter or ImageJ software. The results were expressed as the survival fraction relative to untreated controls.

Annexin V/PI Apoptosis Assay and Western Blotting

HepG2 cells were treated with Danshen extract at concentrations of 0, 15, 60, and 120 µg/mL for 24 hr. After treatment, the cells were harvested using trypsin-EDTA, washed with PBS, and resuspended in Annexin V binding buffer. The cells were stained with 5 µL of Annexin V-FITC and 5 µL of Propidium Iodide (PI) for 15 min in the dark. Apoptosis was analyzed using flow cytometry, with FITC and PI fluorescence measured at excitation/emission wavelengths of 488/530 nm and 535/617 nm, respectively. The cells were categorized as live (Annexin$^-$/PI$^-$), early apoptotic (Annexin$^+$/PI$^-$), late apoptotic (Annexin$^+$/PI$^+$), or necrotic (Annexin$^-$/PI$^+$).

Western blotting

For Western blotting, treated HepG2 cells were lysed in RIPA buffer containing protease inhibitors, and the protein concentration was quantified using a BCA assay. 30 µg of protein per lane were separated on a 10% SDS-PAGE gel and transferred to PVDF membranes. The membranes were blocked with 5% non-fat milk for 1 hr and then incubated overnight at 4°C with primary antibodies against STAT3 (1:1000), HSP90AA1 (1:1000), HSP90AB1 (1:1000), and β-actin (1:2000) as a loading control. The membranes were incubated with HRP-conjugated secondary antibodies (1:5000) for 1 hr, and the bands were detected using ECL reagent. The band intensities were quantified using ImageJ software.

Statistical Analysis

All experiments were performed in triplicate, and the data were analyzed using ANOVA followed by Tukey's post-hoc test, with a significance level of $p < 0.05$.

RESULTS

Screening and Selection of Phytochemicals

Initial screening using the TCMSP database led to the identification of a total of 202 compounds. The selection criteria included a bioavailability (BioAva) of ≥55%, a Drug-Likeness (DL) score of ≥0.18, and a CaCo-2 permeability score of ≥-0.4. This screening reduced the number of compounds to 14. Further refinement was performed by removing compounds with non-identifiable SMILES structures in the PubChem database, leaving 11 compounds. Toxicity analysis based on hepatotoxicity, cytotoxicity, mutagenicity, and carcinogenicity further narrowed the list to 9 compounds. Finally, target identification reduced the number to 8 compounds only (Table 1). The complete study design adopted for the current research work is depicted as a flow chart in Figure 1.

Target Screening and Selection

A total of 904 targets were predicted using SuperPred, along with 4 confirmed targets. Additionally, 700 targets were identified using SwissTargetPrediction (Supplementary Tables S1 and S2). The SuperPred targets were filtered to retain only those with a probability score of ≥70%, reducing the number to 305. After removing duplicates, 114 targets remained. Combining these with the SwissTargetPrediction results (1 target) and the 4 confirmed targets, a total of 119 targets were screened for*S. miltiorrhiza*. Further removal of duplicates eliminated 4 genes, resulting in a

IN PRESS

final list of 115 targets. Separately, 19,097 genes were retrieved from GeneCards, which were filtered to 1,241 genes based on a GeneCards Inferred Functionality Score (GIFTS) of >60. Finally, 74 common genes were identified across all datasets.

PPI network

The eight compounds identified in the screening process yielded 74 common targets associated with liver cancer (Figure 2A). For PPI network analysis, these targets were uploaded to the STRING database (Figure 2B). With 74 nodes and 160 edges, the PPI network has a very significant PPI enrichment p-value of <1.0e-16, an average node degree of 4.32, and a clustering coefficient of 0.465. Using Cytoscape, the network was further displayed, and hub genes were found by using the CytoHubba plugin to determine their centrality and connectedness within the network (Figure 3A). The top hub genes identified included STAT3, HSP90AA1, HSP90AB1, TLR4, STAT1, HIF1A, NFKB1, MAPK1, PIK3R1, and MTOR, which are likely to play critical roles in the molecular mechanisms underlying liver cancer (Figure 3B).

Enrichment analysis

The GO enrichment analysis for targets Danshen in liver cancer reveals role in multiple key processes. The BP highlighted responses to oxidative stress, chemical stimuli, and metabolic regulation, indicating the role of environmental and metabolic stress in cancer progression (Figure 4A). The CC enrichment showed involvement in vesicular transport, plasma membrane

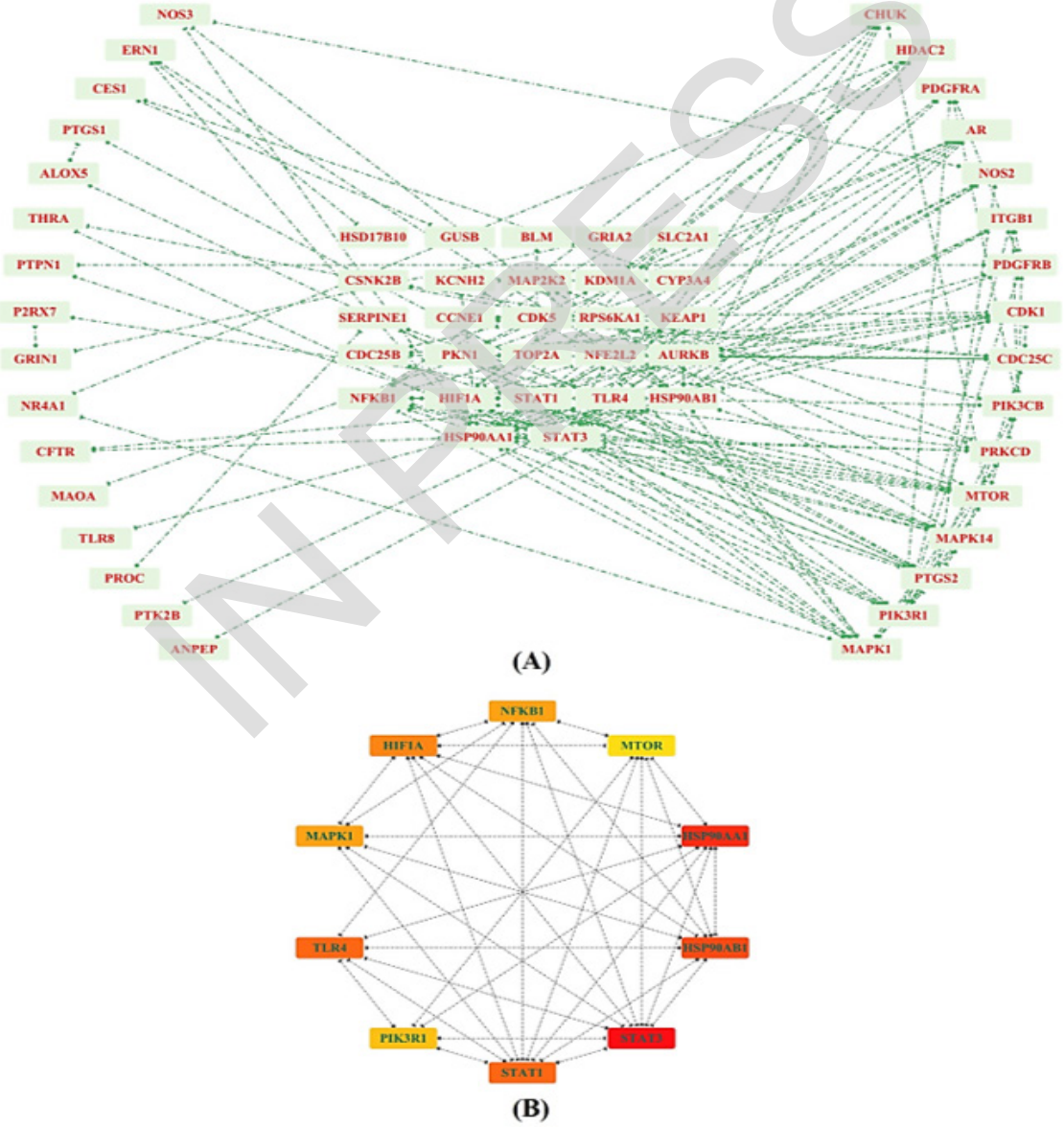


Figure 3: A: Visualization of the PPI network using Cytoscape, highlighting hub genes identified by the CytoHubba plugin. B: Top hub genes (STAT3, HSP90AA1, HSP90AB1, TLR4, STAT1, HIF1A, NFKB1, MAPK1, PIK3R1, and MTOR) identified based on connectivity and centrality within the PPI network.

IN PRESS

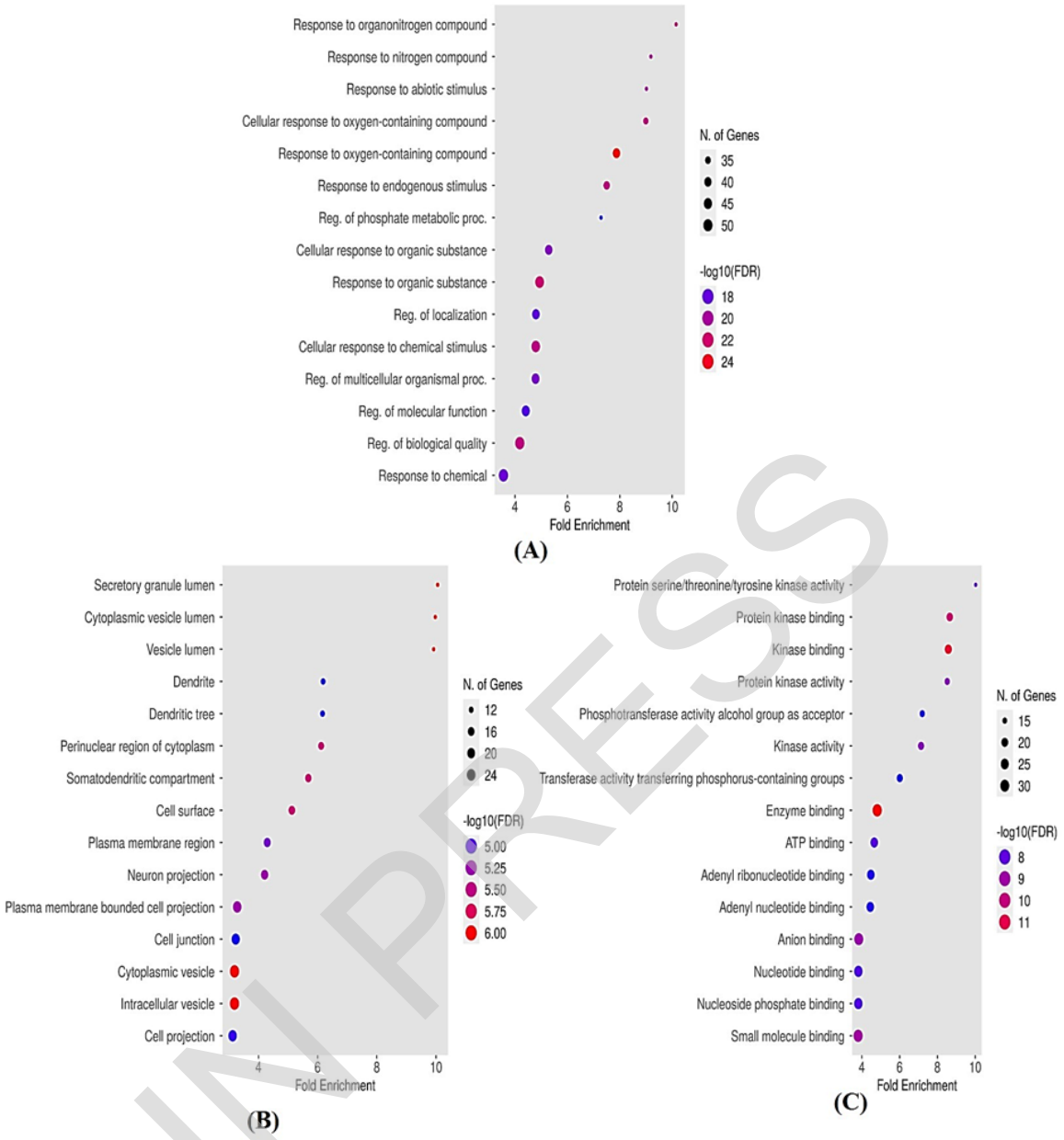


Figure 4: A: GO BP enrichment analysis showing responses to oxidative stress, chemical stimuli, and metabolic regulation. B: GO CC enrichment analysis highlighting vesicular transport, plasma membrane regions, and neuron projections. C: GO MF enrichment analysis identifying kinase activity, ATP binding, and enzyme interactions.

regions, and neuron projections, suggesting altered cellular communication and microenvironment interactions (Figure 4B). The MF analysis identifies significant enrichment in kinase activity, ATP binding, and enzyme interactions, emphasizing the role of dysregulated signaling and energy metabolism in liver cancer (Figure 4C).

The KEGG pathway enrichment analysis of hub genes associated with liver cancer, depicted via a Sankey plot (Figure 5), underscores pivotal signaling pathways implicated in tumorigenesis. Significantly enriched pathways included the PI3K-Akt and HIF-1 signaling pathways and pathways in cancer, bearing critical interplay in regulating survival, proliferation, and angiogenesis during hepatocarcinogenesis. Enrichment of pathways such as the Toll-like receptor signaling and PD-L1/PD-1 checkpoint further implicates immune evasion mechanisms and inflammatory responses in the progression of liver cancer. Metabolic dysregulation is also evident, as highlighted by the enrichment of pathways like the AGE-RAGE signaling pathway in diabetic complications and central carbon metabolism in cancer, suggesting a profound connection between metabolic disturbances and liver tumor development. The chemical carcinogenesis-receptor activation pathway emphasizes the contribution of environmental and chemical exposures to liver cancer etiology. Additionally, the enrichment of pathways related to viral infections, including Kaposi sarcoma

IN PRESS

and Hepatitis B-associated herpesvirus infection, reaffirms their well-documented roles as significant risk factors for hepatocellular carcinoma.

Further, to visualize the significance of Danshen in liver cancer treatment, the whole network was created, including its shared targets with liver cancer and enriched KEGG pathways (Figure 6).

Expression analysis of top ranked hub targets using GEPIA2

The GEPIA2 outcomes for STAT3, HSP90AA1, and HSP90AB1 in liver hepatocellular carcinoma identifies unique expression patterns and prognostic significance. STAT3 expression is not significantly different between tumor and normal tissues, is consistent across tumor stages, and is not significantly correlated with overall or disease-free survival, indicating it is perhaps not a critical prognostic factor (Figure 7). HSP90AA1 is significantly overexpressed in tumors but is not significantly different across stages. Increased HSP90AA1 expression is correlated with worse overall survival (p=0.0024, HR=1.7) but not disease-free survival, suggesting its value as a prognostic marker for survival (Figure 8). Concomitantly, HSP90AB1 is highly overexpressed in cancers and demonstrates a stage-specific fluctuation (p=0.0318), and its high expression is associated with a trend towards worse overall survival (p=0.05, HR=1.4) and disease-free survival (p=0.074, HR=1.3) (Figure 9). These observations indicate that although STAT3 would not be a highly significant prognostic marker, HSP90AA1 and HSP90AB1 may potentially be prognostically relevant in LIHC, especially for overall survival.

Hub genes involvement in TME

The TIMER outcome plots indicate that all three genes, STAT3, HSP90AA1, and HSP90AB1, exhibit positive partial correlations with the infiltration levels of key immune cell types (Figure 10). This indicates elevated expression of each gene is frequently correlated with enhanced immune-cell-infiltration rather than decreased infiltration. STAT3 has a markedly high positive connection with macrophages and CD4 T cells, suggesting its potential significance in the recruitment or activation of these cell

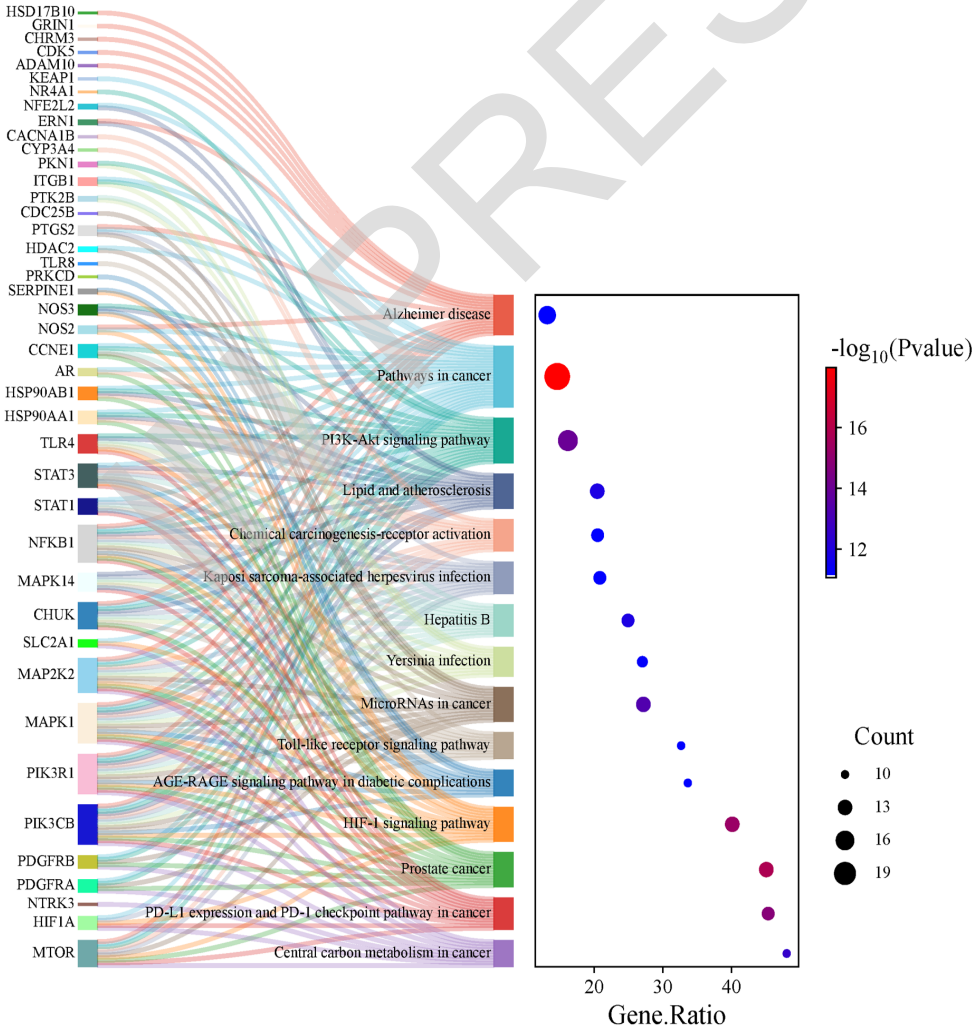


Figure 5: KEGG pathway enrichment analysis of hub genes associated with liver cancer, visualized as a Sankey plot, highlighting key pathways such as PI3K-Akt signalling, HIF-1 signalling, and immune-related pathways.

PRESS

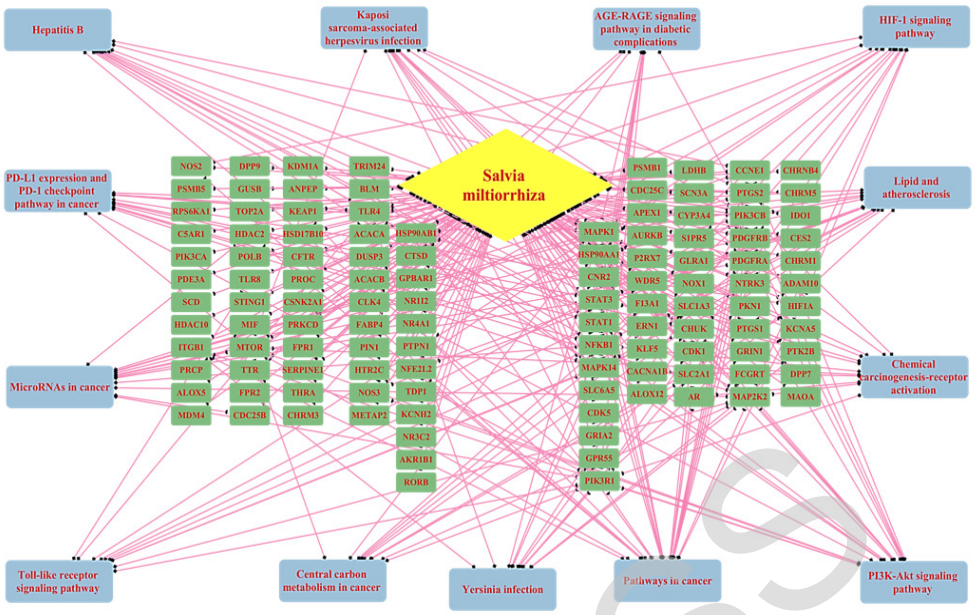


Figure 6: Integrated network of Danshen's shared targets with liver cancer and enriched KEGG pathways, illustrating its potential therapeutic mechanisms.

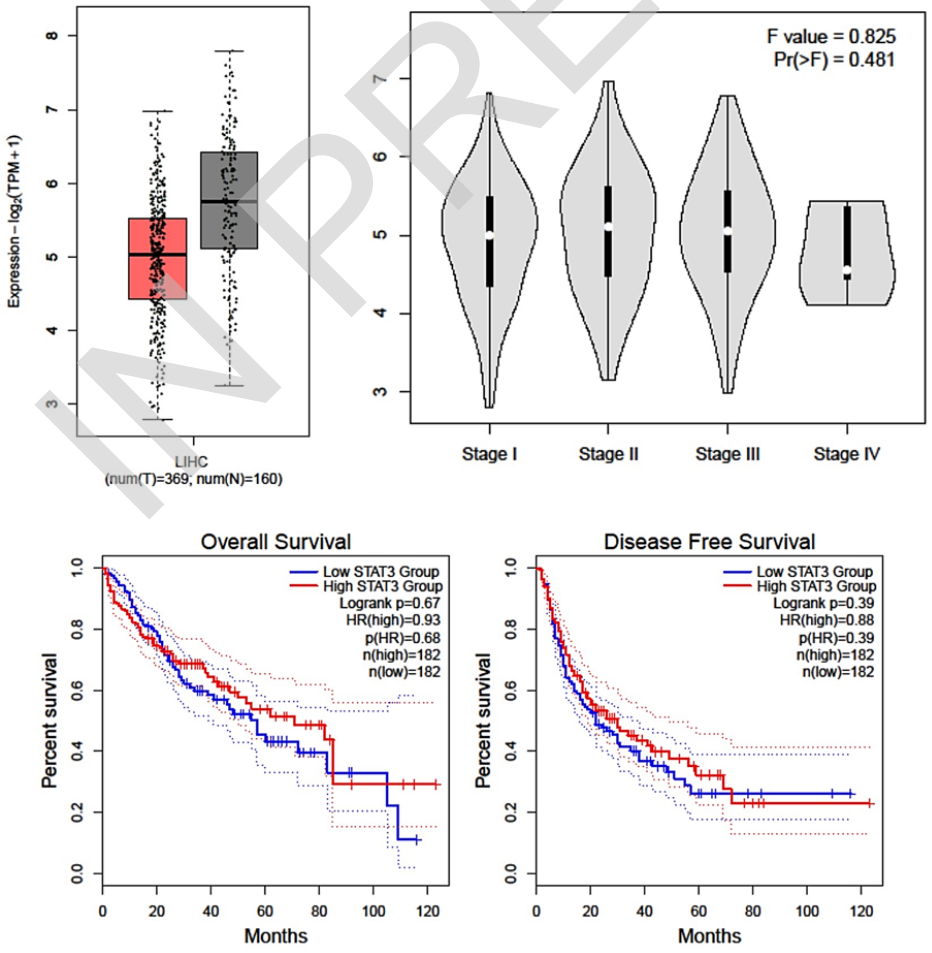


Figure 7: GEPIA2 analysis of STAT3 expression in Liver Hepatocellular Carcinoma (LIHC), showing no significant differences between tumor and normal tissues or correlation with survival.

IN PRESS

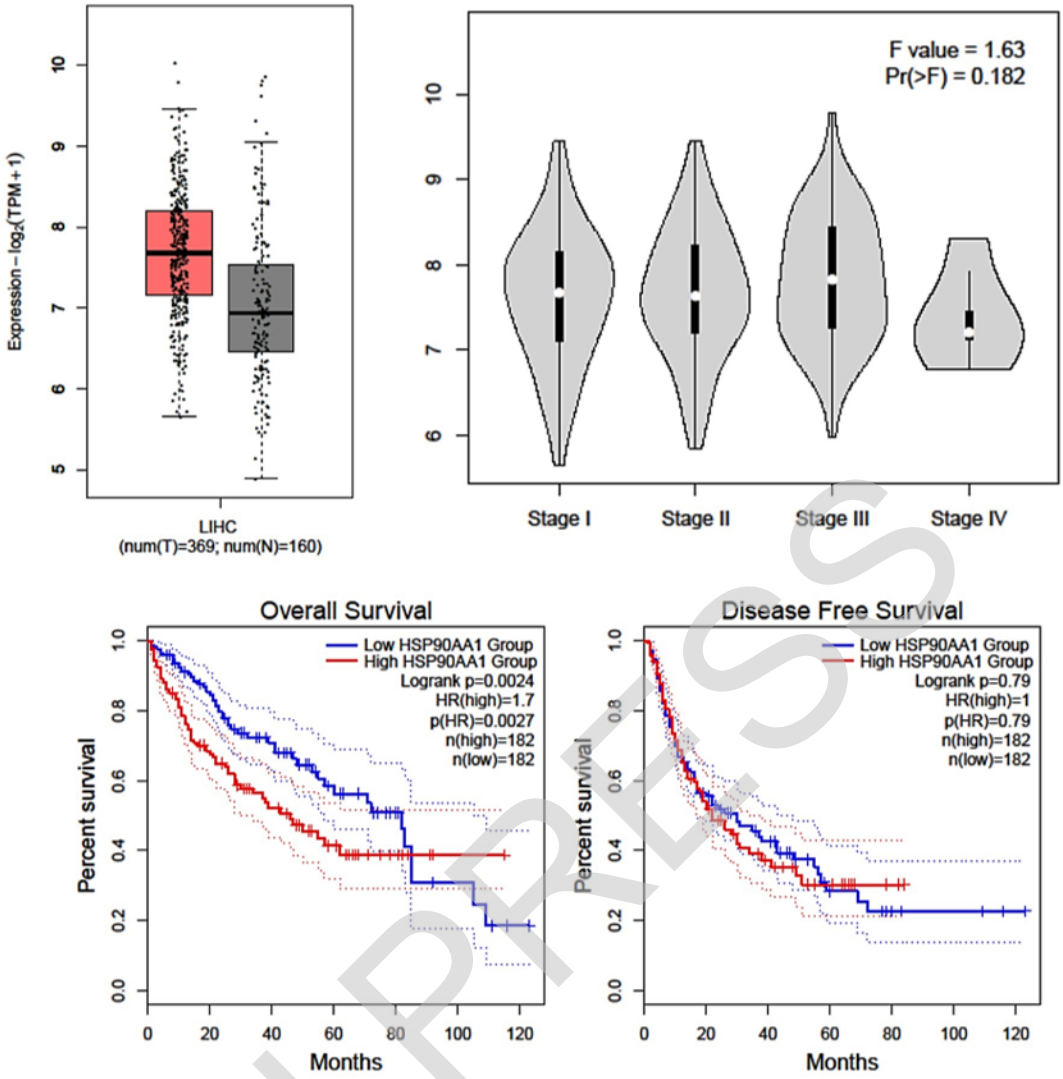


Figure 8: GEPIA2 analysis of HSP90AA1 expression in LIHC, demonstrating significant overexpression in tumors and correlation with worse overall survival.

types. Similarly, HSP90AA1 and HSP90AB1 exhibit significant positive correlations across all assessed immune groups, indicating a potentially extensive pro-immune or immune-supportive influence inside the tumor microenvironment.

Molecular docking for validation of hub genes

The molecular docking results using CB-Dock2 revealed strong interactions between phytochemicals from Danshen (Compound A and Przewalskin b) and hub genes (STAT3, HSP90AA1, and HSP90AB1). Compound A exhibited binding affinities (Vina scores) of -7.0, -9.0, and -9.2 for STAT3, HSP90AA1, and HSP90AB1, respectively, while Przewalskin b showed slightly stronger binding to STAT3 (-7.5) and comparable affinities to HSP90AA1 (-9.1) and HSP90AB1 (-9.1) (Table 2 and Figure 11). The cavity volumes of HSP90AA1 (2038 Å^3) and HSP90AB1 (2023 Å^3) and STAT3 (479 Å^3 and 730 Å^3), facilitated stable binding. Additionally, Discovery Studio was used to generate 2D interaction diagrams, which detailed key molecular associations such as hydrogen-bonding, hydrophobic interactions, and potential pi-pi stacking or salt bridges, providing a mechanistic understanding of the binding stability (Figure 11). These results suggest that Compound A and Przewalskin b are promising candidates for modulating HSP90AA1 and HSP90AB1, with slightly weaker but still significant interactions with STAT3, highlighting their potential therapeutic relevance.

The extract induces cytotoxicity

The MTT assay demonstrated that Danshen extract exhibited selective cytotoxicity against HepG2 cells while showing minimal toxicity toward THLE-2 cells (Figure 12). At concentrations of 15, 30, 60, and 120 µg/mL, Danshen extract significantly reduced the viability of HepG2 cells in a dose-dependent manner, with the highest concentration (120 µg/mL) reducing cell viability to 8% compared to the untreated control. In contrast, THLE-2 cells remained largely less affected, with cell viability above 45%

IN PRESS

Table 2: Docking results for Compound A and Przewalskin b to the top 3 hub genes using CB-Dock2.

Complex	Pocket ID	Docking Score	Binding site (Å³)	Binding center (x, y, z)	Docking size (x, y, z)
Compound A-STAT3	C3	-7.0	479	16, 11, 18	23, 23, 23
Przewalskin b-STAT3	C2	-7.5	730	5, 32, 20	20, 20, 20
Compound A-HSP90AA1	C1	-9.0	2038	7, 35, 24	23, 23, 23
Przewalskin b-HSP90AA1	C1	-9.1	2038	7, 35, 24	26, 20, 20
Compound A-HSP90AB1	C1	-9.2	2023	7, 10, 25	23, 23, 23
Przewalskin b-HSP90AB1	C1	-9.1	2023	7, 10, 25	26, 20, 20

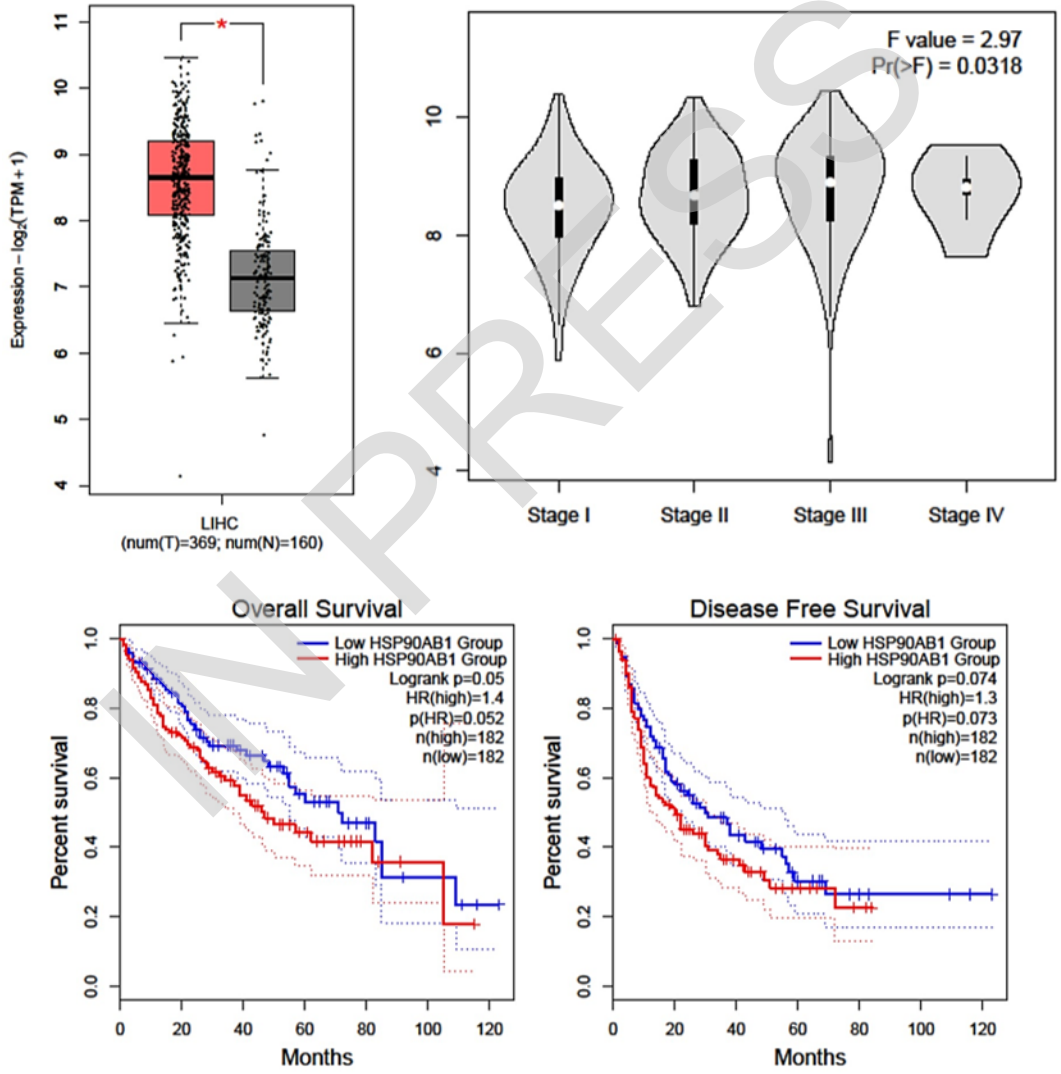


Figure 9: GEPIA2 analysis of HSP90AB1 expression in LIHC, showing stage-specific fluctuations and trends toward overall and disease-free survival.

at higher concentrations, confirming the selective anticancer activity of Danshen extract.

Clonogenic Assay for HepG2 Cells

The clonogenic assay revealed that Danshen extract significantly has a dose-dependent effect in reducing HepG2 cells' capacity to form colonies (Figure 13A). At administration dosages of 15, 60,

IN PRESS

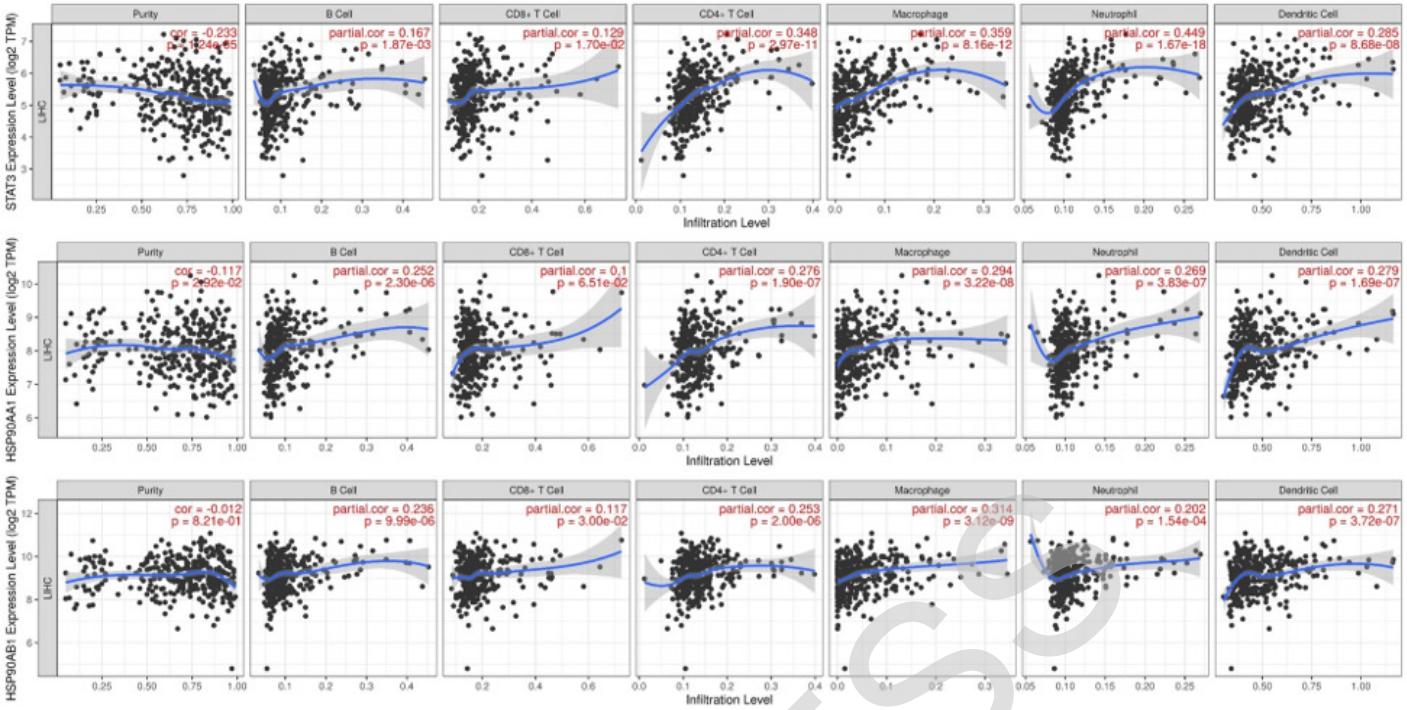


Figure 10: TIMER analysis of STAT3, HSP90AA1, and HSP90AB1, showing positive correlations with immune cell infiltration levels in the tumor microenvironment.

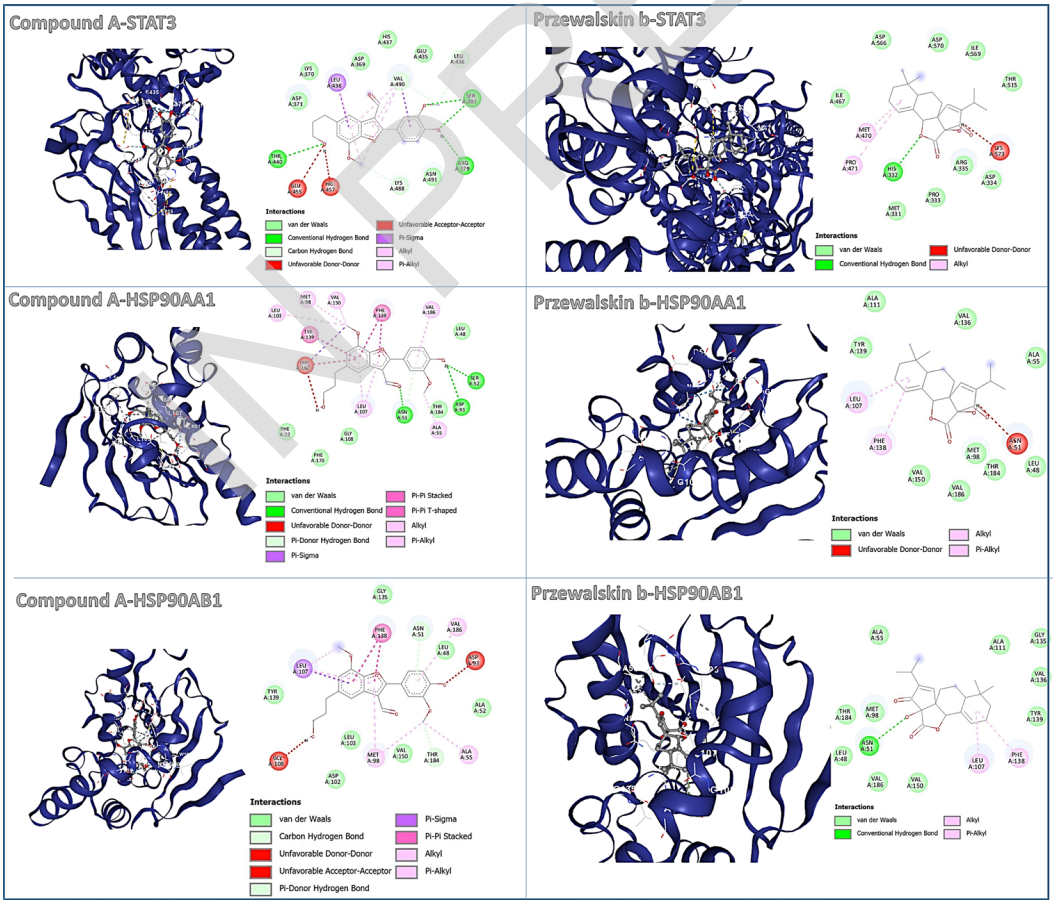


Figure 11: Molecular docking results of Danshen phytochemicals (Compound A and Przewalskin b) with hub genes (STAT3, HSP90AA1, and HSP90AB1), including 2D interaction diagrams generated using Discovery Studio.

NPRESS

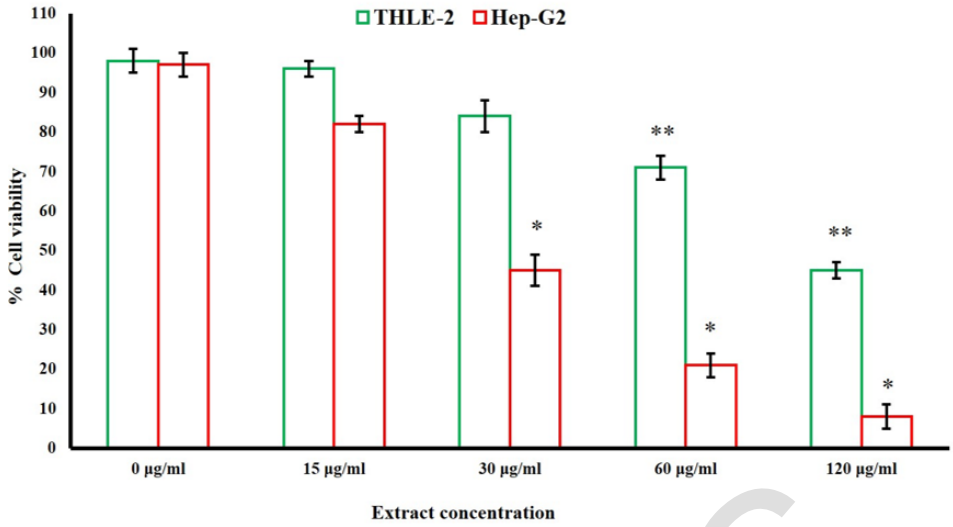


Figure 12: MTT assay results showing selective cytotoxicity of Danshen extract against HepG2 cells, with minimal toxicity toward THLE-2 cells. Experiments were performed in triplicate, and results were shown as SD.

and 120 µg/mL, the survival of HepG2 cells decreased to 395, 176 and 53 in number, respectively, compared to the untreated control (Figure 13B). Colonies treated with 120 µg/mL of Danshen extract were sparse and significantly smaller, indicating potent inhibition of cell proliferation and long-term survival.

Annexin V/PI Apoptosis Assay

The Danshen extract brought about a dose-dependent apoptotic death in HepG2 cells (Figure 14A). At 60 µg/mL, the Annexin$^+$/PI$^-$ cell percentage (early apoptotic cells) increased to 15.6%, while late apoptotic cells (Annexin$^+$/PI$^+$) accounted for 24.5% of the population. At the highest concentration (120 µg/mL), the proportion of Annexin$^+$/PI$^-$ cells rose to 29.7% and 34.3%, respectively, with a corresponding decrease in live cells (Annexin$^-$/PI$^-$) (Figure 14B). These results indicate that Danshen extract promotes apoptosis-mediated death in HepG2 cells.

Danshen extract led to downregulation of STAT3, HSP90AA1, and HSP90AB1 expression in HepG2 cells

The Danshen extract led to a dose-dependent downregulation of the expression levels of STAT3, HSP90AA1 and HSP90AB1 in Hep-G2 cells. As compared to the untreated control, the Danshen extract led to decreased expression of all these proteins; although the effect was much more pronounced in case of STAT3 and HSP90AB1. The highest inhibition was seen at 120 µg/mL concentration of the extract. These *in vitro* results are in full agreement with the network pharmacology results which hint towards the involvement of these hub targets in the anticancer action of Danshen extract (Figure 15).

DISCUSSION

Cancer is a complicated illness that arises from changes in genes and molecules that interfere with regular cellular processes, resulting to uncontrolled proliferation, metastasis/angiogenesis, and resistance to apoptosis.[22] Among the key molecular players implicated in tumorigenesis, STAT3, HSP90AA1, and HSP90AB1 have emerged as crucial regulators of cancer progression. These genes play significant roles in cellular signaling, protein stabilization, and stress response, making them essential in various malignancies, including HCC. Their dysregulation in cancer is often linked to oxidative stress, chronic inflammation, and metabolic variations, contributing to cancer initiation, advancement, and therapeutic resistance.[23]

STAT3 is a key transcription factor that becomes activated through phosphorylation by JAKs, RTKs, and non-receptor kinases like SRC.[24] Once activated, phosphorylated STAT3 translocates and dimerizes into the nucleus, thereby regulates transcription of genes modulating cell survival, proliferation, immune evasion, and angiogenesis. In various cancers, such as lung, breast, colorectal, and hematological malignancies, STAT3's persistent activation leads to enhanced tumor growth and resistance to apoptosis.[25] In HCC, STAT3 plays a particularly crucial role due to its involvement in inflammation-driven tumorigenesis.[26] Chronic liver diseases such as cirrhosis, and hepatitis B/C induce persistent activation in IL-6/STAT3 signaling axis, indorsing cellular proliferation, angiogenesis, and inhibition of immune surveillance.[26] Moreover, STAT3 is implicated in hepatic fibrosis by modulating hepatic stellate cells, which contribute to the fibrotic environment that precedes liver cancer.[27] Additionally, STAT3 drives metabolic reprogramming in hepatocytes, altering glucose metabolism and favouring conditions conducive to tumor growth.[28] Importantly, its activation is associated with sorafenib resistance, the first-line treatment for advanced HCC, highlighting STAT3 as a potential therapeutic target.

Heat Shock Proteins (HSPs) serve as molecular chaperones that regulate protein folding, prevent protein aggregation, and maintain proteostasis under stress conditions.[29] Among them, HSP90AA1 and HSP90AB1, which encode different isoforms

IN PRESS

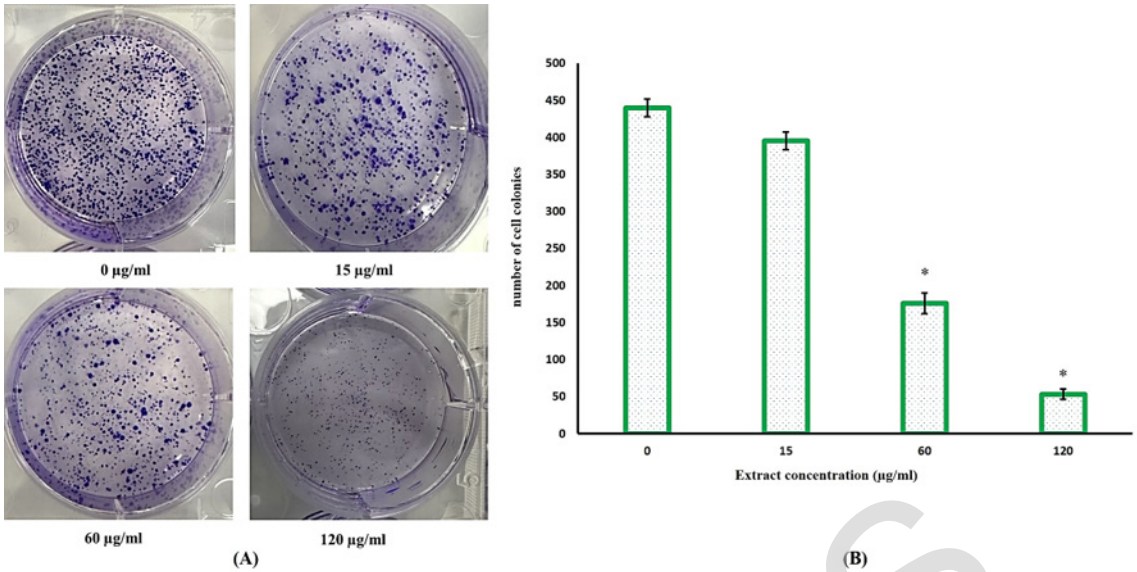


Figure 13: A: Clonogenic assay images demonstrating dose-dependent inhibition of HepG2 colony formation by Danshen extract. B: Quantification of colony numbers showing reduced survival fractions at increasing concentrations of Danshen extract.

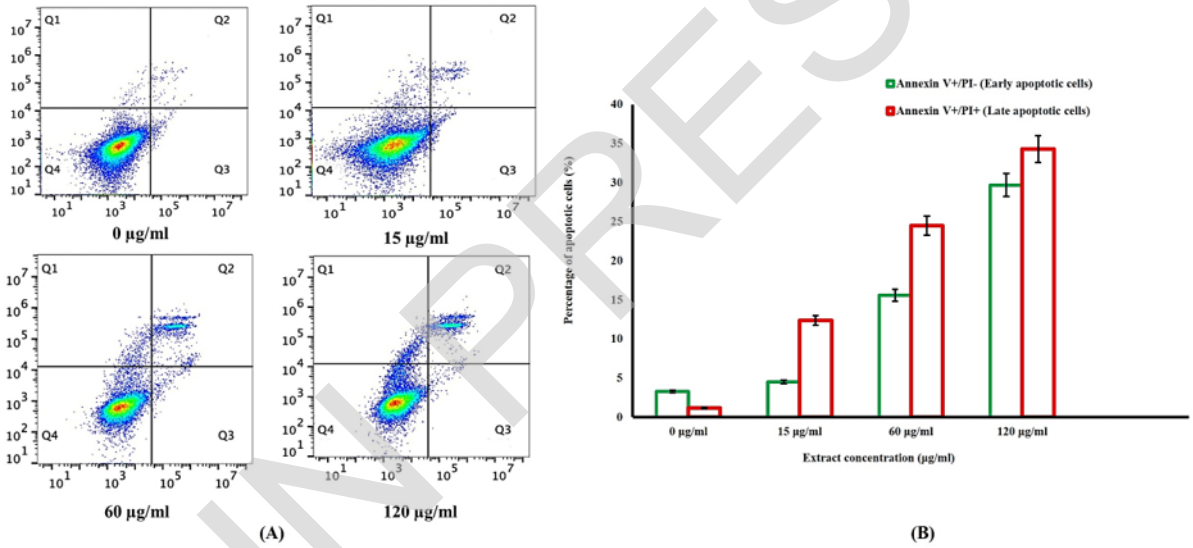


Figure 14: A: Flow cytometry plots of Annexin V/PI staining showing apoptosis induction in HepG2 cells treated with Danshen extract. B: Quantification of early and late apoptotic cells, demonstrating dose-dependent increases in apoptosis.

IN PRESS

of HSP90, have emerged as crucial regulators of oncogenic pathways. HSP90AA1 is the inducible form, upregulated under cellular stress, while HSP90AB1 is constitutively expressed and maintains basal proteostasis.[30] Both isoforms are frequently overexpressed in cancers, where they stabilize multiple oncogenic proteins, including receptor tyrosine kinases (EGFR, HER2), transcription factors (HIF-1α, STAT3), and kinases (AKT, RAF, CDK4), thereby promoting tumor growth, metastasis, and resistance to apoptosis.[31]

In HCC, HSP90 isoforms contribute significantly to disease progression by stabilizing oncogenic proteins and preventing their degradation. HSP90AA1 is particularly involved in JAK2/STAT3 signaling, a key axis in liver cancer development, as well as in AKT/mTOR and RAF/MEK/ERK pathways, which drive proliferation and survival.[32,33] Furthermore, HSP90-mediated stabilization of VEGF enhances angiogenesis, ensuring sustained tumor growth by promoting blood vessel formation.[34] However, HSP90AB1 plays a crucial role in protecting hepatocytes from proteotoxic stress caused by chronic liver disease and oxidative damage, allowing malignant cells to survive under adverse conditions.[35] HSP90 also contributes to Epithelial-to-Mesenchymal-Transition (EMT), one crucial process in metastasis linked to chemotherapy resistance in HCC by stabilizing proteins involved in drug resistance mechanisms.[36]

STAT3, HSP90AA1, and HSP90AB1 are crucial oncogenic drivers in various malignancies, including HCC. STAT3 orchestrates

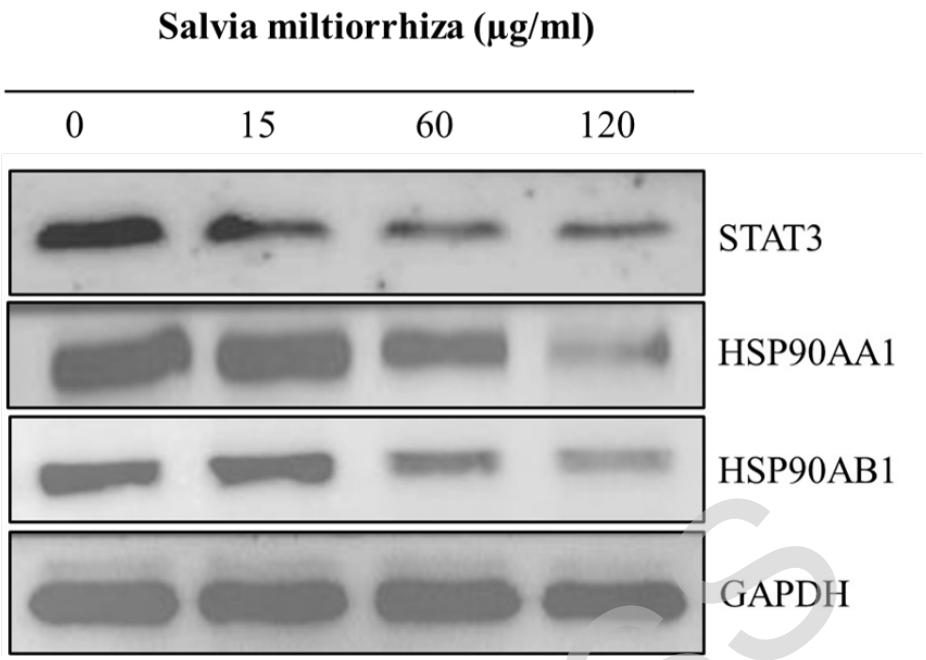


Figure 15: A: Western blot images showing downregulation of STAT3, HSP90AA1, and HSP90AB1 protein expression in HepG2 cells treated with Danshen extract. B: Quantification of protein expression levels, highlighting significant reductions at 60 µg/mL and 120 µg/mL concentrations.

tumor-promoting inflammatory signaling, while HSP90 isoforms stabilize critical oncogenic proteins, ensuring sustained tumor survival and proliferation.[37,38] Their involvement in key oncogenic pathways makes them promising therapeutic targets, especially in combination with existing therapies. Further research into their molecular interactions, inhibitors, and potential biomarkers could open the door to more efficient and customized treatment strategies for liver cancer and other malignancies.

Network pharmacology analysis revealed their association with crucial oncogenic pathways, particularly the PI3K-Akt, HIF-1, and PD-L1/PD-1 signaling pathways, highlighting their role in tumor survival, immune evasion, and metabolic regulation. Molecular docking studies confirmed strong interactions between selected phytochemicals and hub genes STAT3, HSP90AA1, and HSP90AB1, further supporting their potential in modulating key oncogenic mechanisms. Experimental validation demonstrated that Danshen extract exhibited selective cytotoxicity against HepG2 cells, significantly inhibiting colony formation and inducing apoptosis. Additionally, Western blotting confirmed the downregulation of STAT3, HSP90AA1, and HSP90AB1, reinforcing the extract's role in targeting critical molecular pathways in hepatocellular carcinoma.

Several recent studies highlight the anticancer potential of *Salvia miltiorrhiza* (Danshen) and its phytochemicals against hepatocellular carcinoma. Tanshinones, such as tanshinone IIA, cryptotanshinone, dihydrotanshinone, and tanshinone I, have shown selective cytotoxicity and synergy with chemotherapy, while also inhibiting proliferation and inducing apoptosis via PI3K/Akt/mTOR and MAPK pathways in cell and animal models.[39,40] Additionally, *Salvia miltiorrhiza* polysaccharides have demonstrated immunomodulatory effects, enhancing T cell and NK cell responses and regulating cytokine expression to suppress liver tumor growth *in vivo*.[41] Together, these findings support Danshen's multi-targeted therapeutic roles in HCC and its promise for integrative cancer treatment.

CONCLUSION

Eight *Salvia miltiorrhiza* phytochemicals showed anti- HCC potential via ADME, toxicity, and target prediction. Network pharmacology identified *STAT3, HSP90AA1*, and *HSP90AB1* in PI3K-Akt, HIF-1, and PD-L1/PD-1 pathways, linked to oxidative stress, metabolism, and immune evasion. Molecular docking confirmed strong binding of Compound A and Przewalskin B to hub genes. *In vitro*, HepG2 cytotoxicity, low THLE-2 toxicity, colony formation inhibition, and apoptosis were dose-dependent. Western blotting validated *STAT3, HSP90AA1*, and *HSP90AB1* downregulation. These findings highlight the therapeutic potential of Danshen in liver cancer, warranting further *in vivo* and clinical validation.

ACKNOWLEDGEMENT

Not applicable.

ABBREVIATIONS

TCM: Traditional Chinese Medicine (TCM); **PPI:** Protein-Protein Interaction; **GO:** Gene Ontology; **KEGG:** Kyoto Encyclopedia of Genes and Genomes; **GEPIA:** Gene Expression Profiling Interactive Analysis; **MTT:**

IN PRESS

3- (4,5-dimethylthiazol-2-yl)-2,5-diphenyltetrazolium bromide; **MASH:** Metabolic dysfunction-associated steatohepatitis; **TCMSP:** TCMSP - Traditional Chinese Medicine Systems Pharmacology; **TCM-ID:** Traditional Chinese Medicine Information Database; **HCC:** Hepatocellular Carcinoma; **DL:** Drug Likeness; **GIFTS:** GeneCards Inferred Functionality Score; **STRING:** Search Tool for the Retrieval of Interacting Genes/ Proteins; **BP:** Biological Process; **MF:** Molecular Function; **CC:** Cellular Component.

CONFLICT OF INTEREST

The authors declare that there is no conflict of interest.

FUNDING

No funding was received for this work.

SUMMARY

This study investigates the anti-liver cancer potential of *Salvia miltiorrhiza* (Danshen) using network pharmacology, molecular docking, and *in vitro* experiments. From 202 phytochemicals screened via the TCMSP database, eight compounds were selected based on bioavailability, drug-likeness, and toxicity profiles. These compounds targeted 115 potential proteins, with 74 overlapping with liver cancer-related genes from GeneCards. Protein-protein interaction analysis highlighted 10 hub genes, including STAT3, HSP90AA1, and HSP90AB1. Enrichment analyses indicated involvement in PI3K-Akt, HIF-1, and PD-L1/PD-1 pathways. Molecular docking revealed strong binding affinities of Compound A and Przewalskin b to STAT3, HSP90AA1, and HSP90AB1. *In vitro* assays on HepG2 cells confirmed dose-dependent cytotoxicity, reduced clonogenic survival, and apoptosis induction. Western blot analysis validated downregulation of STAT3 and HSP90 proteins, supporting their role in tumor suppression. These findings suggest Danshen's therapeutic potential against liver cancer, warranting further *in vivo* and clinical studies.

REFERENCES

1. Li X, Ramadori P, Pfister D, Seehawer M, Zender L, Heikenwalder M. The immunological and metabolic landscape in primary and metastatic liver cancer. Nature Reviews Cancer. 2021;21(9):541-57.
2. Huang DQ, Singal AG, Kono Y, Tan DJ, El-Serag HB, Loomba R. Changing global epidemiology of liver cancer from 2010 to 2019: NASH is the fastest growing cause of liver cancer. Cell metabolism. 2022;34(7):969-77.
3. Man S, Luo C, Yan M, Zhao G, Ma L, Gao W. Treatment for liver cancer: From sorafenib to natural products. European journal of medicinal chemistry. 2021;224:113690.
4. Zhao L, Zhang H, Li N, Chen J, Xu H, Wang Y, Liang Q. Network pharmacology, a promising approach to reveal the pharmacology mechanism of Chinese medicine formula. Journal of Ethnopharmacology. 2023;309:116306.
5. Xin WA, Zi-Yi WA, Zheng JH, Shao LI. TCM network pharmacology: a new trend towards combining computational, experimental and clinical approaches. Chinese journal of natural medicines. 2021;19(1):1-1.
6. Nogales C, Mamdouh ZM, List M, Kiel C, Casas AI, Schmidt HH. Network pharmacology: curing causal mechanisms instead of treating symptoms. Trends in pharmacological sciences. 2022;43(2):136-50.
7. Jiang YL, Xun Y. Molecular mechanism of *Salvia miltiorrhiza* in the treatment of colorectal cancer based on network pharmacology and molecular docking technology. Drug design, development and therapy. 2024: 425-41.
8. Zhang Y, Xin G, Zhou Q, Yu X, Feng L, Wen A, Zhang K, Wen T, Zhou X, Wu Q, He H. Elucidating the distinctive regulatory effects and mechanisms of active compounds in *Salvia miltiorrhiza* Bunge via network pharmacology: Unveiling their roles in the modulation of platelet activation and thrombus formation. Toxicology and Applied Pharmacology. 2024;484:116871.
9. Huang J, Zhang J, Sun C, Yang R, Sheng M, Hu J, Kai G, Han B. Adjuvant role of *Salvia miltiorrhiza* bunge in cancer chemotherapy: A review of its bioactive components, health-promotion effect and mechanisms. Journal of Ethnopharmacology. 2024;318:117022.
10. Li Y, Zhang X, Li Y, Yang P, Zhang Z, Wu H, Zhu L, Liu Y. Preparation methods, structural characteristics, and biological activity of polysaccharides from *Salvia miltiorrhiza*: A review. Journal of Ethnopharmacology. 2023;305:116090.
11. Luo L, Xue J, Shao Z, Zhou Z, Tang W, Liu J, Hu H, Yang F. Recent developments in *Salvia miltiorrhiza* polysaccharides: isolation, purification, structural characteristics and biological activities. Frontiers in Pharmacology. 2023;14:1139201.
12. Xie F, Zhang B, Dai S, Jin B, Zhang T, Dong F. Efficacy and safety of *Salvia miltiorrhiza* (*Salvia miltiorrhiza* Bunge) and ligustrazine injection in the adjuvant treatment of early-stage diabetic kidney disease: A systematic review and meta-analysis. Journal of Ethnopharmacology. 2021;281:114346.
13. Ye Z, Liu Y, Song J, Gao Y, Fang H, Hu Z, Zhang M, Liao W, Cui L, Liu Y. Expanding the therapeutic potential of *Salvia miltiorrhiza*: a review of its pharmacological applications in musculoskeletal diseases. Frontiers in Pharmacology. 2023;14:1276038.
14. Li H, Hu P, Zou Y, Yuan L, Xu Y, Zhang X, Luo X, Zhang Z. Tanshinone IIA and hepatocellular carcinoma: A potential therapeutic drug. Frontiers in Oncology. 2023;13:1071415.
15. Tao XM, Li D, Zhang C, Wen GH, Wu C, Xu YY, Kan Y, Lu WP, Ding HY, Yang Y. Salvianolic acid B protects against acute and chronic liver injury by inhibiting Smad2C/L phosphorylation. Experimental and therapeutic medicine. 2021;21(4):1.
16. Banerjee P, Kemmler E, Dunkel M, Preissner R. ProTox 3.0: a webserver for the prediction of toxicity of chemicals. Nucleic Acids Research. 2024; 52(W1):W513-20.
17. Gallo K, Goede A, Preissner R, Gohlke BO. SuperPred 3.0: drug classification and target prediction—a machine learning approach. Nucleic Acids Research. 2022; 50(W1):W726-31.
18. Gfeller D, Grosdidier A, Wirth M, Daina A, Michielin O, Zoete V. SwissTargetPrediction: a web server for target prediction of bioactive small molecules. Nucleic acids research. 2014; 42(W1):W32-8.
19. Szklarczyk D, Kirsch R, Koutrouli M, Nastou K, Mehryary F, Hachilif R, Gable AL, Fang T, Doncheva NT, Pyysalo S, Bork P. The STRING database in 2023: protein-protein association networks and functional enrichment analyses for any sequenced genome of interest. Nucleic acids research. 2023; 51(D1):D638-46.
20. Ge SX, Jung D, Yao R. ShinyGO: a graphical gene-set enrichment tool for animals and plants. Bioinformatics. 2020;36(8):2628-9.
21. Liu Y, Yang X, Gan J, Chen S, Xiao ZX, Cao Y. CB-Dock2: Improved protein-ligand blind docking by integrating cavity detection, docking and homologous template fitting. Nucleic acids research. 2022; 50(W1):W159-64.
22. Siegel RL, Miller KD, Fuchs HE, Jemal A. Cancer statistics, 2021. CA: a cancer journal for clinicians. 2021;71(1):7-33.
23. Pei M, Xu N, Li J, Liu X, Zhang L, Xiao W, Yu Z, Yang P, Peng Y, Zhang J, Hong L. The LINC00501-HSP90B1-STAT3 positive feedback loop promotes malignant behaviour in gastric cancer cells. Cellular Signalling. 2023;108:110711.
24. Xu J, Lin H, Wu G, Zhu M, Li M. IL-6/STAT3 is a promising therapeutic target for hepatocellular carcinoma. Frontiers in oncology. 2021;11:760971.
25. Wang X, Hu R, Song Z, Zhao H, Pan Z, Feng Y, Yu Y, Han Q, Zhang J. Sorafenib combined with STAT3 knockdown triggers ER stress-induced HCC apoptosis and cGAS-STING-mediated anti-tumor immunity. Cancer letters. 2022;547:215880.
26. Xu J, Lin H, Wu G, Zhu M, Li M. IL-6/STAT3 is a promising therapeutic target for hepatocellular carcinoma. Frontiers in oncology. 2021;11:760971.
27. Zhao J, Qi YF, Yu YR. STAT3: A key regulator in liver fibrosis. Annals of Hepatology. 2021;21:100224.
28. Kilanczyk E, Banales JM, Jurewicz E, Milkiewicz P, Milkiewicz M. p-STAT3 is a PDC-E2 interacting partner in human cholangiocytes and hepatocytes with potential pathobiological implications. Scientific Reports. 2021;11(1):21649.
29. Hu C, Yang J, Qi Z, Wu H, Wang B, Zou F, Mei H, Liu J, Wang W, Liu Q. Heat shock proteins: Biological functions, pathological roles, and therapeutic opportunities. MedComm. 2022;3(3):e161.
30. Boopathy LR, Jacob-Tomas S, Alecki C, Vera M. Mechanisms tailoring the expression of heat shock proteins to proteostasis challenges. Journal of Biological Chemistry. 2022;298(5).
31. Zuo WF, Pang Q, Zhu X, Yang QQ, Zhao Q, He G, Han B, Huang W. Heat shock proteins as hallmarks of cancer: insights from molecular mechanisms to therapeutic strategies. Journal of Hematology and Oncology. 2024;17(1):81.
32. Niu M, Song S, Su Z, Wei L, Li L, Pu W, Zhao C, Ding Y, Wang J, Cao W, Gao Q. Inhibition of heat shock protein (HSP) 90 reverses signal transducer and activator of transcription (STAT) 3-mediated muscle wasting in cancer cachexia mice. British Journal of Pharmacology. 2021;178(22):4485-500.

IN PRESS

33. Liu B, Qian D. Hsp90α and cell death in cancers: a review. Discover Oncology. 2024;15(1):1-0.
34. Sager RA, Khan F, Toneatto L, Votra SD, Backe SJ, Woodford MR, Mollapour M, Bourboulia D. Targeting extracellular Hsp90: A unique frontier against cancer. Frontiers in Molecular Biosciences. 2022;9:982593.
35. Maiti S, Picard D. Cytosolic Hsp90 isoform-specific functions and clinical significance. Biomolecules. 2022;12(9):1166.
36. Singh P, Jay DG. The role of eHSP90 in extracellular matrix remodeling, tumor invasiveness, and metastasis. Cancers. 2024;16(22):3873.
37. Albakova Z, Mangasarova Y. The HSP immune network in cancer. Frontiers in immunology. 2021;12:796493.
38. Niu M, Song S, Su Z, Wei L, Li L, Pu W, Zhao C, Ding Y, Wang J, Cao W, Gao Q. Inhibition of Heat Shock Protein (HSP) 90 reverses signal transducer and activator of transcription (STAT) 3-mediated muscle wasting in cancer cachexia mice. British Journal of Pharmacology. 2021;178(22):4485-500.
39. Lee WY, Cheung CC, Liu KW, Fung KP, Wong J, Lai PB, Yeung JH. Cytotoxic effects of tanshinones from *Salvia miltiorrhiza* on doxorubicin-resistant human liver cancer cells. Journal of natural products. 2010;73(5):854-9.
40. Li H, Hu P, Zou Y, Yuan L, Xu Y, Zhang X, Luo X, Zhang Z. Tanshinone IIA and hepatocellular carcinoma: A potential therapeutic drug. Frontiers in Oncology. 2023;13:1071415.
41. Liu Y, Wu J, Hao H. Antitumor immunostimulatory activity of the traditional Chinese medicine polysaccharide on hepatocellular carcinoma. Frontiers in Immunology. 2024;15:1369110.

Cite this article: Xu Y, Wang Y, Mao Y, Ma Y. Multi-Omics and *in silico* Study of Anticancer Potential of *Salvia miltiorrhiza* (Danshen in Traditional Chinese Medicine) in Liver Cancer Cells: Metabolomics, Proteomics, Transcriptomics, *In silico* Molecular Docking, and *in vitro* Analysis. Indian J of Pharmaceutical Education and Research. 2027;61(1):10.5530/ijper.20262532.

IN PRESS